The narrow-spectrum anthelmintic oxantel is a potent agonist of a novel acetylcholine receptor subtype in whipworms

Tina V. A. Hansen[1,2*], Susanna Cirera[1], Cédric Neveu[2], Kirstine Calloe[1], Dan A. Klaerke[1*] and Richard J Martin[3]

[1]Department of Veterinary and Animal Sciences, Faculty of Health and Medical Sciences, University of Copenhagen, Dyrlaegevej 100, 1870 Frederiksberg C, Denmark.

[2]INRAE, UMR Infectiologie et Santé Publique, Nouzilly, France.

[3]Department of Biomedical Sciences, College of Veterinary Medicine, Iowa State University, Ames, IA, USA.

[*] alstrup@sund.ku.dk, dk@sund.ku.dk

Abstract

In the absence of efficient alternative strategies, the control of parasitic nematodes, impacting human and animal health, mainly relies on the use of broad-spectrum anthelmintic compounds. Unfortunately, most of these drugs have a limited single-dose efficacy against infections caused by the whipworm, *Trichuris*. These infections are of both human and veterinarian importance. However, in contrast to a wide range of parasitic nematode species, the narrow-spectrum anthelmintic oxantel has a high efficacy on *Trichuris spp*. Despite this knowledge, the molecular target(s) of oxantel within *Trichuris* is still unknown. In the distantly related pig roundworm, *Ascaris suum*, oxantel has a small, but significant effect on the recombinant homomeric **N**icotine-sensitive ionotropic acetylcholine receptor (*N*-AChR) made up of five ACR-16 subunits. Therefore,

we hypothesized that in whipworms, a putative homolog of an ACR-16 subunit, can form a functional oxantel-sensitive receptor. Using the pig whipworm *T. suis* as a model, we identified and cloned a novel ACR-16-like receptor subunit and successfully expressed the corresponding homomeric channel in *Xenopus laevis* oocytes. Electrophysiological experiments revealed this receptor to have distinctive pharmacological properties with oxantel acting as a full agonist, hence we refer to the receptor as an *O*-AChR subtype. Pyrantel activated this novel *O*-AChR subtype moderately, whereas classic nicotinic agonists surprisingly resulted in only minor responses. We demonstrated that the novel *Tsu*-ACR-16-like receptor is indeed a target for oxantel and is more responsive to oxantel than the ACR-16 receptor from *A. suum*. These finding most likely explain the high sensitivity of whipworms to oxantel, and highlights the importance of the discovery of additional distinct receptor subunit types within *Trichuris* that can be used as valuable screening tools to evaluate the effect of new synthetic or natural anthelmintic compounds.

Author Summary

The human whipworm, *Trichuris trichiura*, is an intestinal parasitic nematode infecting approximately 289.6 million people globally, primarily children living in developing countries. Chronic *T. trichiura* infection may cause dysentery, growth stunting and decreased cognitive performance. Whipworm infections are notoriously difficult to control with most available anthelmintics, including those commonly used in mass drug administration programs. Recently performed randomised controlled trials with whipworm-infected humans, have reported superior efficacies of oxantel, a classic, narrow-spectrum anthelmintic, developed for the treatment of *Trichuris* infections. Despite this knowledge, the molecular target(s) of oxantel within the whipworm has not been identified. In this study, we used the whipworm from pigs as a model and identified a receptor, which was explored using the *Xenopus* oocyte expression system. We

demonstrated that this receptor is highly responsive to oxantel, and therefore a major target of oxantel within *Trichuris*. In addition, we discovered that this receptor-type is distinctive and only present in the ancient group of parasitic nematodes, Clade I, which also includes the important zoonotic parasite *Trichinella*. Our findings, explain the specific mode of action of oxantel and open the way for additional characterization of similar receptor subtypes in other medically or veterinary important parasitic nematodes of Clade I.

1. Introduction

The human whipworm, *Trichuris trichiura*, is a Clade I parasitic nematode [1] and one of the Soil Transmitted Helminths (STHs) that is estimated to infect 289.6 million people globally, primarily those living in the tropics and subtropics [2]. Trichuriasis is rarely fatal, but chronically affects the health and nutritional status of the host [3,4], and is known to be notoriously difficult to treat using current anthelmintic drugs (e.g. albendazole and mebendazole) [5–12]. The extensive use of anthelmintics in livestock has led to widespread anthelmintic resistance (AR) to all the major drug classes [13]. Therefore AR in human parasitic nematodes is a concern where decreased susceptibility to albendazole has already been reported for both *T. trichiura* [14] and the human roundworm, *Ascaris lumbricoides* [15].

Oxantel, is a cholinergic agonist [16], and a *m*-oxyphenol analogue of pyrantel which was developed in 1972 [17] and marketed as a veterinary anthelmintic in 1974 for the treatment of *Trichuris* [18]. Early clinical trials reported oxantel to be effective against *T. trichiura* infections [19,20] and recent studies show that oxantel is superior to single-dose albendazole and mebendazole [21,22], which are currently recommended by the WHO for the control of STHs [23]. Cholinergic agonists [16] exert their effect by paralyzing the worms, which are subsequently killed or expelled from the host [24]. This effect is mediated by nicotinic acetylcholine receptors (nAChRs) [24] that are either heteromeric

or homomeric five-subunit ligand-gated ion channels expressed in neuronal, muscle and non-neuronal cell membranes [25,26]. nAChRs of parasitic nematodes have been separated into different pharmacological subtypes based on their sensitivities to a range of cholinergic anthelmintics. Patch-clamp recordings of muscle cells isolated from the pig roundworm *A. suum*, have revealed that their muscle nAChRs are preferentially activated either by levamisole (L), nicotine (N) or bephenium (B), and correspondingly are described as *L*-, *N*-, and *B*- AChRs subtypes [27]. Oxantel is classified as an agonist which is selective for the *N*-AChR subtypes [16]. The *N*-AChR subtypes from the model nematode *Caenorhabditis elegans* and the distantly related pig parasite *A. suum* are homomeric receptors made of the ACR-16 subunits [28,29]. Both of these ACR-16 receptors have a low, but significant sensitivity to oxantel [29,30].

The high sensitivity of *Trichuris* spp. to oxantel has previously been speculated to be due to an nAChR subtype present in *Trichuris* spp. that differs from nAChRs present in other intestinal parasitic nematodes [16]; we hypothesized that a potential homolog of ACR-16 in *Trichuris* could be a target of oxantel within this species.

Here we describe the functional characterization of a novel AChR subtype from the pig whipworm *T. suis* with a high sensitivity to oxantel and distinctive pharmacological properties. This homomeric receptor, referred to as an *O*-AChR subtype, is made of a divergent subunit specific to Clade I nematode species that is only distantly related to ACR-16 from nematode species belonging to other clades. Our results provide new insights about the mode of action of oxantel, its high efficacy on whipworms, and the divergent anthelmintic sensitivity of whipworms.

2. Results

2.1. *Identification of T. suis sequences related to the ACR-16 group.*

Using the *C. elegans* ACR-16 deduced amino-acid sequences as a query, tBLASTn search against *T. suis*, *T. muris* and *T. trichiura* genomic data available in WormBase-ParaSite (version WBPS14; http://parasite.wormbase.org/) allowed the identification of two distinct hits for each species sharing identities ranging from 46% to 47% with the *C. elegans* sequence. Subsequently, a second tBLASTn search against nematodes genomic data available at the NCBI was performed with the retrieved *Trichuris spp*. sequences. Homologies could be identified with either of the *acr-16* or *acr-19* genes from nematode species representative from the nematoda phylum. Using a panel of representative *C. elegans* nAChRs subunits as reference, a phylogenetic analysis including the *Trichuris* spp. and their putative homologs in the closely related species *Trichinella spiralis* was carried out (Fig. 1). *Trichuris* spp. sequences were found to form two distinct clusters. The first one presented a clear orthologous relationship with ACR-19, the second one clustered apart from the other subunits and belonged to the ACR-16 group [31]. An additional analysis, including other related sequences from nematode species representative from the different clades of the nematoda phylum (Suppl. Fig. 1) further confirmed that Clade I nematode species (including *Trichuris* spp.) possess a divergent group of AChR subunit related to the ACR-16 subunit. Consequently, the corresponding sequences from Clade I nematode species were named ACR-16-like.

2.2 Molecular cloning of the Tsu-acr-16-like coding sequence.

In the present study, based on the current knowledge of the original mode of action of oxantel [16,29], we hypothesized that the divergent ACR-16-like from *Trichuris* spp. could represent a preferential target for this narrow-spectrum anthelmintic. Using *T. suis* as a model, we cloned its *acr-16-like* full-length cDNA sequence as a matter of priority and deposited the sequence in GenBank under the accession number MT386096. An alignment of the *Tsu*-ACR-16-like sequence with its closely related counterparts from *T. muris*, *T. trichiura*, *T. spiralis* and *C. elegans* is provided in Fig. 2. The *Tsu-*

ACR-16-like subunit was found to share typical features of nAChR subunits including a predicted signal peptide, a Cys-loop motif, four transmembrane regions (TM1-TM4), and the YxCC motif which characterize an α-type nAChR receptor subunit.

2.2. *Tsu-ACR-16-like subunits form a functional homomeric receptor when co-expressed with the ancillary protein RIC-3 in the Xenopus laevis oocyte.*

Previous studies have shown that *Cel*-ACR-16 and *Asu*-ACR-16 can form functional homomeric receptors when expressed in *X. laevis* oocytes with the ancillary protein RIC-3 [29,32]. Thus, we explored the requirement of RIC-3 for optimizing the putative functional expression of *Tsu-acr-16-like* cRNA in *X. laevis* oocytes. *Xenopus laevis* oocytes were micro injected with *Tsu-acr-16-like* cRNA in combination with *Asu-ric*-3 or *Xle-ric*-3 cRNA. *Tsu-acr-16-like* cRNA or *Asu-ric*-3 cRNA alone as well as non-injected oocytes were used as controls.

The combination of *Tsu-acr-16-like* and *Asu-ric*-3 or *Tsu-acr-16-like* and *Xle-ric*-3 cRNAs led to robust expression of functional receptors responding to 100 µM ACh, which elicited inward currents in the µA range (Fig. 3). The largest currents were measured in oocytes co-injected with *Tsu-acr-16-like* and *Asu-ric*-3 cRNA (mean ± SEM, 7.54 ± 0.74, µA, *n*=32, data not shown); subsequently all other responses were normalized to this. Oocytes co-injection with *Tsu-acr-16-like* and *Xle-ric*-3 cRNA resulted in relatively high current responses (mean ± SEM, 5.0 ± 0.72 µA, *n*=6, data not shown), but oocytes injected with this cRNA combination degraded faster than oocytes injected with *Tsu-acr-16-like* and *Asu-ric*-3 cRNA (data not shown). Non-injected oocytes, or oocytes injected with either *Tsu-acr-16-like* or *Asu-ric*-3 cRNA alone, did not respond to 100 µM ACh, highlighting the need of RIC-3 for the functional expression of the homomeric *Tsu*-ACR-16-like receptor. Representative traces of the inward currents for each injection type, and a bar chart presenting their

mean ± SEM normalized values are shown in Fig. 3. Based on these results, all subsequent recordings were performed on oocytes co-injected with *Tsu-acr-16-like* and *Asu-ric*-3 cRNAs.

2.3. *Oxantel is a potent agonist on the Tsu-ACR-16-like receptor.*

To explore the effect of oxantel and perform a detailed pharmacological characterization of the *Tsu*-ACR-16-like receptor, we used 4 cholinergic anthelmintics (i.e. oxantel, pyrantel, morantel and levamisole) and 5 nAChR agonists (i.e. epibatidine, nicotine, 3-bromocytisine, DMPP and cytisine). Fig. 4 shows the rank order potency series of these drugs, representative traces of the inward currents induced by each of them, the number of oocytes (*n*) used for each agonist, along with a bar chart presenting the normalized mean ± SEM for each drug group. Oxantel was the most potent agonist on the *Tsu*-ACR-16-like receptor and induced a current response even higher than the control response of 100 µM ACh. Pyrantel also induced a relatively high current response, however, the nicotinic agonists: epibatidine, nicotine, 3-bromocytisine, DMPP and cytisine as well as the cholinergic anthelmintics, morantel and levamisole, were the least potent. The rank order potency series for the agonist drugs on the *Tsu*-ACR-16-like receptor when normalized to control oocytes exposed to 100 µM ACh was: oxantel > ACh >>> pyrantel >>> epibatidine > nicotine ~ 3-bromocytosine ~ DMPP ~ morantel ~ cytosine ~ levamisole. Taken together, these observations provide strong evidence that the *Tsu*-ACR-16-like receptor represents the preferential molecular target for oxantel. Interestingly, when exposed to 100 µM ACh for 1-3 min the *Tsu*-ACR-16-like receptor did not show a fast-desensitization kinetics (Suppl. Fig. 2) which is a distinctive characteristic of the *N*-AChR of nematode such as *Asu*-ACR-16 [29] and the ACR-16 from *Parascaris equorum* (*Peq*-ACR-16) [33].

2.4. *Dose-response curve of oxantel and pyrantel*

Oxantel and pyrantel have similar chemical structures (Fig. 5A), but their potencies on the *Tsu*-ACR-16-like receptor were found to be significantly different (Fig. 4). We performed a dose-response study on oxantel and pyrantel to determine their EC_{50} values, their relative maximum current responses, $I_{max,}$ and their Hill slopes, $n_{H.}$ The mean current response of positive control oocytes exposed to 300 µM ACh was used for normalization. Fig. 5B shows representative traces and dose-response relationships of the normalized inward currents (mean ± SEM) induced by different concentrations of oxantel or pyrantel. The EC_{50} ± SE for oxantel (9.49 ± 1.13 µM) was significantly lower than that of pyrantel (148.5 ± 1.19 µM, $P < 0.001$). The relative maximum current response, I_{max} (mean ± SE) was significantly larger for oxantel (86.85 ± 4.63%) than pyrantel (29.41 ± 1.95%, $P = 0.003$), whereas no significant difference was found between the Hill slopes, n_H (mean ± SE), of oxantel (2.51 ± 1.31) and pyrantel (3.13 ± 1.07).

2.5. *Antagonists*

To further characterize the pharmacology of *Tsu*-ACR-16-like receptor, we tested 3 selected antagonists: dihydro-β-erythroidine (DHβE), α-bungarotoxin (α-BTX) and the anthelmintic, derquantel. Fig. 6 shows the effect of 10 µM DHβE and 10 µM derquantel on the *Tsu*-ACR-16-like receptor along with representative current responses. The initial ACh (100 µM) current response of each oocyte was used for normalization, to measure the reduced current responses in the presence of the antagonists. For DHβE, the mean ± SEM inhibition was very small (i.e. 7.60 ± 1.6%) and no inhibition was observed for derquantel (0.16 ± 1.6%). The effect of α-BTX is given in Figure 7A which shows the response-inhibition of the *Tsu*-ACR-16-like receptor to 100 µM ACh when 10 µM α-BTX is applied 10 s before the second application of 100 µM ACh (test oocytes). Fig. 7B shows the effect of the *Tsu*-ACR-16-like receptor when exposed to 100 µM ACh, only (control oocytes). The first current response of 100 µM ACh (ACh1) was used for normalization. Representative current

190 traces along with a bar chart presenting the normalized mean ± SEM of the second and third drug
191 application of test- and control oocytes are given in Fig. 7A and 7B. The 10 µM α-BTX significantly
192 ($P < 0.0001$) reduced the current response of ACh to 8.3 ± 2.4% of the test oocytes (Fig. 7A). This
193 reduction was not observed in the control oocytes (Fig. 7B), thus, when α-BTX was applied 10 s
194 before the second application of ACh, the current response was significantly reduced in test oocytes
195 as compared to control oocytes (Fig. 7A and 7B , $P < 0.0001$).
196
197 **3. Discussion**
198 In the present study, we report the identification and the functional expression of the *Tsu*-ACR-16-
199 like receptor, a novel AChR subtype corresponding to the first specific drug target for oxantel to be
200 reported in any nematode species. In reference to the previously reported *L*-AChR, *N*-AChR, and *M*-
201 AChR (respectively for Levamisole-sensitive, Nicotine-sensitive and Morantel- sensitive –AChR
202 subtypes), we named the novel oxantel-sensitive AChR subtype: the *O*-AChR.
203
204 *The O-AChR is a novel receptor subtype specific to Clade I nematode species with original*
205 *pharmacological properties*
206 Use of screens for *C. elegans* mutants that survive exposure to the broad-spectrum anthelmintics
207 provided a means to decipher their molecular targets in a wide range of nematode species. However,
208 this approach was not helpful for oxantel because the *C. elegans* is insensitive to this drug [34]. The
209 weak, but measurable activity of oxantel on recombinant *N*-AChR from *C. elegans* and *A. suum,*
210 supported the hypothesis that a putative ACR-16 homologs in *Trichuris* species could be involved in
211 an oxantel-sensitive receptor. Williamson et al. [35] reported that only two members from the ACR-
212 16 group could be identified in the genomic data from the Clade I species *T. spiralis*. In agreement
213 with this finding, our search for ACR-16 homologs only retrieved two sequences in each of the

214 *Trichuris* species investigated in the present work. The first one corresponded to the highly conserved
215 AChR subunit encoded by the *acr-19* gene; the second one corresponded to a highly divergent subunit
216 specific to Clade I nematode species designated as ACR-16-like.
217 When co-expressed in the *X. laevis* oocytes with the ancillary protein RIC-3, the ACR-16-like
218 subunits from *T. suis* formed a functional homomeric channel (*O*-AChR) with unexpected
219 pharmacological properties. Indeed, this receptor was highly sensitive to oxantel which is in contrast
220 to the *Asu*-ACR-16 for which a low agonist effect of oxantel has been reported (i.e. <10% of the
221 control ACh current) [29] and to the *Cel*-ACR-16 on which oxantel has an antagonistic effect [30].
222 Likewise, pyrantel had a relatively high effect on the *Tsu-O*-AChR, whereas pyrantel had no agonist
223 effect on *Asu*-ACR-16 [29] or *Cel*-ACR-16, but in contrast, showed an antagonistic effect on the
224 latter, which was ascribed to pyrantel acting as an open channel blocker [28]. In accordance with this
225 assumption, patch-clamp recording studies from isolated *A. suum* muscle cells, show that both oxantel
226 and pyrantel to act as agonists and open channel blockers [36,37]. Another surprising difference
227 between the *Tsu-O*-AChR and the ACR-16 receptors from *A. suum*, *C. elegans* and *P. equorum* is the
228 lack of sensitivity to nicotinic agonists [28,29,33]. Since oxantel has been characterised as an agonist
229 selective for the *N*-subtypes of the ionotropic AChRs [16] which include the ACR-16 receptors, we
230 expected the *Tsu-O*-AChR receptor to be highly sensitive to nicotine, cytosine, 3-bromocytosine,
231 epibatidine and DMPP, but only small current responses were observed using these agonists. Another
232 feature of the *Tsu-O*-AChR receptor is its slow desensitization kinetics, which contrasts with the faster
233 desensitization of the *N*-AChR from *C. elegans* [38], *A. suum* [29] and *P. equorum* [33].
234 Interestingly, we also showed that the antagonist, α-BTX had a potent inhibitory effect on the ACh
235 induced current responses of the *Tsu-O*-AChR whereas *A. suum* [29] and *C. elegans N*-AChR [28]
236 are nearly insensitive to α-BTX. We point out however, that α-BTX only induced a strong inhibitory
237 effect when α-BTX was applied 10 s before the application of ACh suggesting a slow association

238 time of α-BTX. The *Tsu-O*-AChR was virtually insensitive to DHβE and insensitive to derquantel.
239 This also contrasts with the *Asu-N*-AChR which is moderately sensitive to DHβE (~ 65% inhibition)
240 and derquantel (~ 60% inhibition) [29] and the *Cel-N*-AChR which is highly sensitive to DHβE [28].
241 Another notifiable difference is the large current response of the *Tsu-O*-AChR. In the RIC-3
242 experiments we found a mean current response to 100 µM ACh of 7.54 ± 0.74, µA (*n*=32), whereas
243 the current response of *Asu-N*-AChR to 100 µM ACh was 290.6 ± 63.7 nA (*n*=23) [29], and for *Cel-*
244 ACR-16 to 300 µM ACh ~ 400 nA. For comparison, the current responses to 300 µM ACh of the
245 *Tsu-O*-AChR was 12.94 ± 0.77 µA, *n*=24 (mean ± SEM). Taking into consideration variation between
246 studies, (i.e. number of days for receptor expression), the *Tsu-O*-AChR induced a current response
247 approximately 26 and 19 times higher than *Asu-N*-AChR and *Cel-N*-AChR, respectively.
248 Taken together, these results strongly support our hypothesis that *O*-AChR and *N*-AChR represent
249 two distinct class of ionotropic AChR. Despite the important differences, it is noteworthy that there
250 are also similarities between the *O*- and *N*-AChR: both subtypes are not activated by the anthelmintic
251 drugs levamisole or morantel [27-29].
252
253 *Sensitivity to oxantel and pyrantel*
254 Small changes in structure of acetylcholine agonists can have large effects on the selectivity and
255 affinity of nicotinic agonists [39]. Perhaps it is not surprising that pyrantel which was modified by
256 replacing the 2-thiophene moiety with the an *m*-oxyphenol group [17] to produce oxantel has a
257 different pharmacology. Thus, the anthelmintic spectrum of oxantel and pyrantel is very different.
258 Pyrantel is a broad-spectrum anthelmintic with no effect on adult *Trichuris* [17] whereas oxantel is
259 a narrow-spectrum anthelmintic with a potent and selective effect on adult *Trichuris* [19–22]. This
260 spectrum difference has previously raised the question whether a cholinergic receptor subtype

present in *Trichuris* spp. are different from other intestinal nematode parasites [16], which indeed is now strongly supported by our results .

In conclusion, the discovery of the *Tsu-O*-AChR provides new insights for the high efficacy and specificity of oxantel on whipworms, and provide us with an example of an anthelmintic, that due to its narrow-spectrum will have a lower impact on non-target nematode species. The advantage of such an anthelmintic is the reduced risk of inducing anthelmintic resistance in other parasitic nematode species, and a lower impact on the environmental biodiversity after drug expulsion from the host (i.e. primarily animal hosts).

4. Material and methods

4.1. *Ethic statement*

The worm material used in this study was obtained during a previous described study [40] performed at the Experimental Animal Unit, University of Copenhagen, Denmark according to the national regulations of the Danish Animal Inspectorate (permission no. 2015-15-0201-00760). The neurologic tissue from *X. laevis* was obtained from one adult female, which was anaesthetized by submersion into a tricaine solution (ethyl 3-aminobenzoate methanesulfonate, 2g/l) and subsequently decapitated. All procedures involving live material were performed according to the national regulations of the Danish National Animal Experiments Inspectorate (permission no. 2015-15-0201-00560).

4.2. *Drugs*

All drugs except 3-bromocytisine, DHβE, α-BTX and derquantel were purchased at Sigma-Aldrich (Copenhagen, DK). 3-bromocytisine, DHβE and α-BTX were obtained from Tocris Bioscience

(Abingdon, UK) and derquantel was purchased at Cayman Chemicals (Ann Abor, MI, USA). Stock solutions of drugs were made in either Kulori medium or DMSO (100%) and stored at -20 or 5°C (i.e. ACh) until use. Before use, stock solutions were dissolved in Kulori medium with a maximum final concentration of DMSO of 0.1%.

4.3. *Bioinformatics and sequence analysis*

The *Asu*-ACR-16 (accession number AKR16139) and the *Cel*-ACR-16 (accession number NP505207) were used as queries in database searches for *Trichuris suis* ACR-16 (*Tsu*-ACR-16) and ACR-16s from other Clade I parasitic nematodes (i.e. *Trichuris* spp. and *Trichinella spiralis*) in the protein-protein BLAST (BLASTp) service at the National Center for Biotechnology Information (NCBI) service [41]. *Cel*-ACR-16 and *Cel*-ACR-19 were used in an alignment with the identified putative ACR-16 sequences from Clade I parasitic nematodes. The accession numbers of the sequences used for the alignment are:

Caenorhabditis elegans*:** ACR-16 NP505207, ACR-19 NP_001129756. ***Trichuris suis*:** putative ACR-16 KFD48832.1 putative ACR-19 KFD70086.1. ***Trichuris trichiura: putative ACR-16 CDW52185; putative ACR-19 CDW53523. ***Trichuris muris***: putative ACR-16 WBGene00290200; putative ACR-19 WBGene00291941. ***Trichuris spiralis***: putative ACR-16 KRY38920.1, putative ACR-19 KRY27533.1.

Signal peptide was predicted using the SignalP 4.1 server [42] and the transmembrane regions were predicted using the TMHMM version 2 server [43]. Deduced amino-acid sequences were aligned using MUSCLE Phylogenetic analysis was performed on deduced amino-acid sequence. Maximal likelihood phylogeny reconstruction was performed using PhyML V20120412

(https://github.com/stephaneguindon/phyml-downloads/releases) and the significance of internal tree branches was estimated using bootstrap resampling of the dataset 100 times. The accession numbers sequences used for the analysis are:

Caenorhabditis elegans*:** ACR-7 NP_495647; ACR-8 NP_509745; ACR-9 NP_510285; ACR-10 NP_508692; ACR-11 NP_491906; ACR-12 NP_510262; ACR-14 NP_495716; ACR-15 NP_505206; ACR-16 NP_505207; ACR-19 NP_001129756; EAT-2 NP_496959; LEV-1 NP_001255705; UNC-29 NP_492399; UNC-38 NP_491472; UNC-63 NP_491533. ***Haemonchus contortus: ACR-16 MH806893. ***Soboliphyme baturini***: acr-16-like VDP07835.1. ***Steinernema glaseri***: ACR-16 KN173365.1. ***Steinernema feltiae***: ACR-19 KN166031.1. ***Toxocara canis***: ACR-16 VDM44142.1; ACR-19 VDM36763.1. ***Parascaris equorum*:** ACR-26 KP756902; ACR-27 KP756903. ***Trichuris suis*:** ACR-16-like KFD48832; ACR-19 KFD70086.. ***Trichuris muris*:** ACR-16-like WBGene00290200; ACR-19 WBGene00291941. ***Trichuris trichiura*:** ACR-16-like CDW52185; ACR-19 CDW53523. ***Trichinella spiralis:*** ACR-16-like KRY38920.1; ACR-19 KRY27533.

4.4. *cDNA synthesis*

Worm material was kept in RNA later (Sigma-Aldrich, Copenhagen, DK) at -20°C until use. Total RNA was extracted from whole adult *T. suis* males and females using TRIzol LS Reagent (Invitrogen™). For each isolation, 15 worms were used. The RNA was DNAse treated using DNase I, Amplification Grade (Invitrogen). The whole brain of one *X. laevis* frog was used to extract RNA using Tri™ Reagent®; (MRC. Inc; US) and M tubes in an OctoMacs homogenizer machine (Milteny, Germany) following the manufacturer' protocol. The isolated RNA was DNAse treated using the RNeasy MinElute Cleanup kit (Qiagen, Germany). The quantity and quality of RNA from *T. suis* and *X. laevis* was assessed by OD measurement in a Nanodrop spectrophotometer (Thermo Scientific,

Demark) and by visual inspection in an agarose gel (1%). First strand cDNA was synthesised from 2.5 µg of total RNA from *T. suis* and brain RNA from *X. laevis* using SuperScript IV VILO Master Mix (Invitrogen™) according to manufacturer's protocol.

4.5. *PCR and cloning of a full-length T. suis ACR-16 subunit and Xle-RIC-3*

To amplify the full-length coding sequence of the *Tsu-acr-16-like* subunit, a specific primer pair, containing the *Bam*HI and the *Not*I restriction enzyme sites and 5 additional nucleotides (*Tsu-acr-16*-F-5'- GAATC-*Bam*HI-ATGCGGCCGATAATTTTCCTC-3' and *Tsu-acr-16*-R- 5'-ACGTT *Not*I TCACACAGTTAAATGGGGAGAAC-3') were designed using the putative *Tsu-acr-16-like* sequence in Wormbase under gene number M514_10316. The specific primer pair used to amplify the *Xle-ric*-3 sequence are described elsewhere [32]. Restriction enzyme sites (*Bam*HI and *Not*I) were included to facilitate ligation into the expression vector pXOOM [44] which was linearized with the restriction enzymes *Bam*HI and *Not*I. PCR amplifications were performed with Platinum SuperFi Green PCR Master Mix (Invitrogen) following the manufacturer' recommendations. Amplicons were evaluated by gel electrophoresis, digested with *Bam*HI and *Not*I, purified with QIAquick Gel Extraction Kit (Qiagen), cloned into pXOOM and sequenced. A positive clone of *Tsu-acr-16-like* subunit and *Xle-ric-3* was selected and linearized with the restriction enzyme *Nhe*I before *in vitro* transcription using the mMessage mMachine T7 Transcription Kit (Ambion). The cRNA was purified using MEGAclear (Thermo Scientific, Demark). Quantity and quality of cRNA was evaluated by OD measurement in a Nanodrop spectrophotometer (Thermo Scientific, Demark) and by visual inspection in an agarose gel (1%).

4.6. *Microinjection of Xenopus laevis oocytes*

354 *Xenopus laevis* oocytes were obtained from EcoCyte Bioscience (Castrop-Rauxel, Germany) and kept
355 at 19°C in Kulori medium (90 mM NaCl, 4 mM KCl, 1 mM $MgCl_2$, 1 mM $CaCl_2$, 5 mM HEPES,
356 pH:7.4) until injection. Oocytes were injected with 50 nl of cRNA in RNAse-free water using a
357 microinjector (Nanojet, Drummond Broomal, PA, USA). To test *ric*-3 effects on the receptor
358 expression, 25 ng *Tsu-acr-16-like* cRNA was injected alone or with either 5 ng *Asu-ric*-3 or 5 ng *Xle-*
359 *ric*-3 cRNA. To exclude endogenous nAChR expression induced by *Asu-ric*-3, 5 ng *Asu-ric*-3 was
360 injected alone. These amounts of cRNA were chosen in order to compare the drug-potency results of
361 the *Tsu*-ACR-16-like receptor with that of *Asu*-ACR-16[29]. Only half (i.e. 12.5 ng *Tsu-acr-16-like*
362 cRNA and 2.5 ng *Asu-ric*-3) was used for the dose-response curves and antagonist analysis. To allow
363 for receptor expression, the injected oocytes were incubated in Kulori medium at 19°C for 3-7 days
364 and the Kulori medium was changed daily.
365
366 4.7. *Two-electrode voltage clamp of Xenopus laevis oocytes*
367 Two-electrode voltage-clamp (TEVC) recordings were obtained using an Oocyte Clamp Amplifier
368 OC-725 B (Warner Instruments Corp., USA) connected to an Axon Digidata® 1440A digitizer (Axon
369 Instruments, Molecular Devices, USA) and was performed at ~19°C under continuous flow of Kulori
370 medium with the oocytes clamped at -60 mV. Data were sampled at 2 kHz using the pClamp 10.4
371 acquisition software (Axon Instruments, Molecular Devices, USA). The microelectrodes were pulled
372 from glass capillaries (TW 120.3, World precision instruments, USA) on a programmable
373 micropipette puller (Narishige, Japan). The resistance when filled with 3 M KCl ranged from 0.5 to
374 1.5 MΩ. Ag/AgCl reference electrodes were connected to the bath with agar bridges. For a minimum
375 of 4 hours prior to recording, all oocytes were incubated in BAPTA-AM at a final concentration of
376 100 µM to chelate intracellular Ca^{2+} ions and hereby prevent activation of endogenous calcium

activated chloride channels during recordings. Recordings from non-injected oocytes were used as negative controls.

4.8. *Drug-potency-tests*

All agonists were used at a final concentration of 100 µM and were tested in 3-4 experiments using 3-4 different batches of oocytes batches. For each experiment, 6 oocytes were tested per drug. For each experiment, 6 oocytes were exposed to 100 µM ACh for 10 s, and all other responses in the same experiment, were normalized to the mean response of these controls. Initial experiments showed a consistent decrease in the response to 100 µM ACh when applied repeatedly, even after washing periods for up to 5 min between agonist applications. Therefore, each drug was tested on oocytes not previously exposed to ACh (100 µM). The total number of oocytes examined per drug was: $n = 23$ for oxantel, $n = 16$ for pyrantel, $n = 15$ for epibatidine, $n = 16$ for nicotine, $n = 15$ for 3- bromocytisine, $n = 16$ for DMPP, $n = 17$ for morantel, $n = 17$ for cytisine and $n = 15$ for levamisole. Each drug was applied for 10 s followed by wash off until the current had returned to pre-stimulation values.

4.9. *Dose-response studies.*

The dose-response studies were in total performed on 3 different oocyte batches. For oxantel the number of measurements per drug concentration were as follows: 0.3 µM, n=6; 0.1 µM, n=6; 3 µM, n=6; 3 µM, n=6; 10 µM, n=15; 30 µM, n=12; 100 µM, n=13; 300 µM, n=14. For pyrantel n per drug concentration were: 1 µM, n=6; 3 µM, n=6; 10 µM, n=6; 30 µM, n=6; 100 µM, n=15; 300 µM, n=23; 1000 µM, n=12; 3000 µM, n=20. For each experiment, 6 oocytes were exposed to 300 µM ACh for 10 s, and all other responses in the same experiment, were normalized to the mean response of these positive controls. The ACh concentration of 300 µM was used to reach the supposed maximal

400 activation of the *Tsu*-ACR-16-like receptor. Each drug and drug concentration were tested as
401 described for the drug-potency-tests.
402
403 4.10. *Antagonists*
404 The effects of the antagonists DHβE, derquantel and α-BTX (10 µM) were examined in the presence
405 100 µM ACh as previously described for *Asu*-ACR-16 [29]. In short, *X. laevis* oocytes co-injected
406 with *Tsu-acr-16-like*- and *Xle-ric*-3 cRNA were sequentially superfused with ACh for 10 s, then ACh
407 + antagonist for 10 s, and finally with ACh for 10 s. For α-BTX a five-step protocol including a pre-
408 incubation (10 s) with the antagonist (10 µM) was used with ACh (100 µM). *Xenopus laevis* oocytes,
409 co-injected with *Tsu-acr-16-like*- and *Xle-ric*-3 cRNAs, were exposed to: i) a control application of
410 100 µM ACh for 10 s (first application); ii) followed by a wash-off period of 5 min; iii) then by an
411 application of 10 µM α-BTX for 10 s, immediately followed by 100 µM ACh and the continued
412 presence of α-BTX for 10 s (second application); iv) then a wash-off period of 5 min; v) and finally
413 an application of ACh for 10 s (third application). Control oocytes were exposed to ACh for 10 s in
414 3 consecutive steps, each separated by a wash-off period of 5 min. For each antagonist, n=6-8.
415
416 4.11. *Electrophysiological data and statistically analysis*
417 All acquired electrophysiological data were analysed with Clampfit 10.7 (Molecular Devices,
418 Sunnyvale, CA, USA) and GraphPad Prism 8 (GraphPad Software, La Jolla, CA, USA) and from all
419 experiments, peak currents from BAPTA-AM-incubated oocytes were measured after application of
420 drugs. For the auxiliary protein (RIC-3) test, the largest group mean current in response to 100 µM
421 ACh was set to 100%, and all other responses were normalized to this. The relative means were
422 statistical analysed using One-Way ANOVA with a Dunnett's Test and $P < 0.05$ was considered
423 significant. For the drug-potency-test, peak currents of drugs were normalized to the peak current

424 measured in the presence of 100 µM ACh and was expressed as mean ± SEM. Data was tested for
425 normality using the D'Agostino-Pearson normality test. Drug-group means were statistical analysed
426 using One-Way ANOVA with a Turkey's Multiple Comparison Test where $P < 0.05$ was considered
427 significant.
428
429 For the dose-response relationships, and for each experiment, 6 oocytes were exposed to ACh (300
430 µM) for 10 s, and all other drug responses in the same experiment, were normalized to the mean
431 response of these controls. The normalized current as a function of drug concentration allowed fitting
432 the dose-response curves with a Hill equation, using nonlinear regression analysis with a variable
433 slope model in GraphPad Prism 8. The following equation was used:
434
435 $$I_{rel} = I_{min} + (I_{max} - I_{min})/ (1 + 10\text{^}((\text{Log}EC_{50}\text{-}[D])*n_H)),$$
436
437 where I_{rel} is the mean relative current, I_{max}, is the relative current obtained at saturating agonist
438 concentration, I_{min} is the relative current obtained at agonist concentration 0 µM, EC_{50} is the
439 concentration of agonist resulting in 50% of the maximal current response, [D] is the drug
440 concentration and n_H is the Hill coefficient. $I_{max,}$ EC_{50} and n_H were fitted as free parameters whereas
441 $I_{min,}$ was constrained to 0.
442 For the antagonist test with α-BTX, the current response of α-BTX and ACh in the continued presence
443 of α-BTX (second application) was normalized to the first response at 100 µM ACh (first application)
444 which was set to 1. The group mean of the α-BTX response were statistical analysed using One-Way
445 ANOVA with a Dunnett's test.
446
447 **6. Acknowledgement**

448 The study was supported by the Independent Research Fund Denmark (DFF – 4184-00210), the
449 Danish National Advanced Technology Foundation (5184-00048B) and the Lundbeck Foundation
450 (R9-A1131). authors would like to thank Richard Martin at Iowa State University, USA for
451 providing the *Asu*-ACR-16 and *Asu*-RIC-3. RJM is supported by NIH, the National Institute of
452 Allergy and Infectious Diseases grants R01AI047194-17, R21AI092185-01A1 and the E. A.
453 Benbrook Foundation for Pathology and Parasitology. In addition, the authors wish to thank Vibeke
454 Grøsfjeld Christensen at the Veterinary and Animal Sciences, University of Copenhagen for
455 technical assistance.

456

457

458

459 **Figure legends**

460 **Figure 1**

461 Maximum likelihood tree showing relationships of the ACR-16 related acetylcholine receptor
462 (nAChR) subunits from *Trichuris species,* with other *C. elegans and T. spiralis* nAChR subunits.
463 Tree was built upon an alignment of nAChR subunit deduced amino-acid sequences. The tree was
464 rooted with the *Parascaris equorum* ACR-26 and ACR-27 sequences that are absent from *C. elegans*
465 and clade I nematode species (Courtot *et al.* 2018). Scale bar represents the number of substitutions
466 per site. Boostrap values are indicated on branches. Accession numbers for sequences used in the
467 phylogenetic analysis are provided in the Material and Methods section. *C. elegans* nAChR subunit
468 groups are named as proposed by Mongan *et al.* [31], *Cel*, *Tsu*, *Ttr*, *Tmu*, *Tsp* and *Peq* refer to
469 *Caenorhabditis elegans*, *Trichuris suis*, *Trichuris trichiura*, *Trichuris muris* and *Parascaris equorum,*
470 respectively.

471

472 **Figure 2**

473 Amino acid alignment of ACR-16-(like) and ACR-19 subunit sequences from the Clade I parasitic
474 nematodes *Trichuris suis*, *T. trichiura*, *T. muris*, *Trichinella spiralis* and *Caenorhabditis elegans*.
475 Predicted signal peptide sequences are shaded in grey, the Cys-loop, the transmembrane regions
476 (TM1-TM4), and the YxCC motif that characterize an α-subunit are indicated above the sequences.
477 Conserved amino acids between ACR-16-(like) and ACR-19 sequences (dark blue), conserved amino
478 acids between all ACR-16-(like) sequences (red), conserved amino acid between all ACR-19
479 sequences (light green), conserved amino acid between ACR-16-like sequences of Clade I parasitic
480 nematodes and ACR-19 of *C. elegans* (light blue).

481

482 **Figure 3**

Effect of the ancillary protein Resistance-to-cholinesterase (RIC-3) from *Ascaris suum* (*Asu*-RIC-3) and *Xenopus laevis* (*Xle*-RIC-3) on the functional expression of the ACR-16-like nAChR from *Trichuris suis* (*Tsu*-ACR-16-like receptor). Representative sample traces of inward current in response to 100 µM ACh are shown together with a bar chart presenting the relative currents (mean ± SEM). Oocytes injected with *Tsu-acr-16-like*- or *Asu-ric-3* cRNA alone did not respond to 100 µM ACh. The relative current of oocytes co-injected with *Tsu-acr-16-like* and *Asu-ric*-3 cRNA was significantly higher than oocytes injected with *Tsu-acr-16-like* and *Xle-ric*-3 cRNA. $P < 0.05$; significantly different as indicated, Dunnett's test.

Figure 4

The effect of 9 agonists on *Tsu*-ACR-16-like receptor. Representative sample traces and a bar chart (mean ± SEM) show the rank order potency series of 4 cholinergic anthelmintics: oxantel (oxa), pyrantel (pyr), morantel (mor), levamisole (lev) and 5 nAChR agonists: epibatidine (epi), nicotine (nic), 3-bromocytisine (3-bc), dimethylphenylpiperazinium (DMPP) and cytisine (cyt). $P < 0.05$; significantly different as indicated; Turkey's multiple comparison test.

Figure 5a

Chemical structure of oxantel and pyrantel. Oxantel: free drawing after https://pubchem.ncbi.nlm.nih.gov/compound/oxantel#section=2D-Structure. Pyrantel: free drawing after https://pubchem.ncbi.nlm.nih.gov/compound/pyrantel#section=2D-Structure

Figure 5b

Dose-response curves for oxantel (oxa) and pyrantel (pyr). The current response on *Tsu*-ACR-16-like receptor is normalised to current responses induced by 300 µM ACh and given as mean ±

SEM. The EC_{50} ± SD values were 9.48 ± 1.15 µM for oxa and 152.7 ± 1.20 µM for pyr, the relative maximum current responses, I_{max} were 86.85 ± 4.63% and 29.41 ± 1.95%, and the Hill slope, $n_{H,}$ 2.51 ± 1.30 and 3.13 ± 1.07 for oxa and pyr, respectively.

Figure 6

Effect of the antagonists: dihydro-β-erythroidine (DHβE) and derquantel (der) on *Tsu*-ACR-16-like receptor mediated 100 µM ACh current response. Results are given as normalized mean ± SEM inhibition of the initial current response of 100 µM ACh. DHβE produced an almost insignificant block of the *Tsu*-ACR-16-like receptor mediated ACh response (i.e. 7.60 ± 1.61%) and no effect was observed for der (0.16 ± 1.61%).

Figure 7a and 7b

Effect of the antagonists α-bungarotoxin (α-BTX) on *Tsu*-ACR-16-like receptor mediated 100 µM ACh current response. The first ACh current response (ACh1) is set to 100 for both test- (figure 5a) and control oocytes (figure 5b), and subsequent current responses are given as normalized mean ± SEM inhibition of ACh1. $P < 0.05$; significantly different as indicated, Dunnett's test.

Supplementary figure legends

Supplementary figure 1

Distance tree showing relationships of the ACR-16-like acetylcholine receptor (AChR) subunits from Clade I nematode species, with other AChR subunits from the ACR-16 group from nematode species representative from Clade III, Clade IV, and Clade V.

NJ-Tree was built upon an alignment of AChR subunit deduced amino-acid sequences. The tree was rooted with the *C. elegans* UNC-63 sequence. Scale bar represents the number of substitutions per site. Boostrap values (1000 replicates) are indicated on branches. Accession numbers for sequences used in the analysis are provided in Material and Methods section. Nematode clades refer to Blaxter et al. 1998 [1]. AChR subunit sequences from Clade I species are highlighted in red, AChR subunit sequences from Clade III species are highlighted in blue, AChR subunit sequences from Clade V species are highlighted in pink (in black for *C. elegans*). *Cel*, *Hco*, *Sba*, *Sgl*, *Sfe*, *Tca*, *Tsp*, *Tsu*, *Ttr* and *Tmu* refer to: *Caenorhabitis elegans*, *Haemonchus contortus*, *Soboliphyme baturini*, *Steinernema glaseri*, *Steinernema feltiae*, *Toxocara canis*, *Trichinella spiralis*, *Trichuris suis*, *Trichuris trichiura*, and *Trichuris muris* respectively.

Supplementary figure 2

Desensitization kinetics of *Tsu*-ACR16-like receptor. A representative response of the *Tsu*-ACR16-like receptor to 1 min exposure of 100 µM ACh. The *Tsu*-ACR16-like receptor is characterized by a slow-desensitization kinetic as compared to *Asu*-ACR-16 [29] and *Peq*-ACR-16 [33].

546 **References**

547 1. Blaxter ML, De Ley P, Garey JR, Liu LX, Scheldeman P, Vierstraete A, et al. A molecular
548 evolutionary framework for the phylum Nematoda. Nature. 1998; 392(6671):71-5. doi:
549 10.1038/32160. PMID: 9510248

550

551 2. James SL, Abate D, Abate KH, Abay SM, Abbafati C, Abbasi N, et al. Global, regional, and
552 national incidence, prevalence, and years lived with disability for 354 Diseases and Injuries for
553 195 countries and territories, 1990-2017: A systematic analysis for the Global Burden of
554 Disease Study 2017. Lancet. 2018; 392(10159): 1789–1858. doi:10.1016/S0140-
555 6736(18)32279-7. PMID: 30496104

556

557 3. Stephenson LS, Latham MC, Ottesen EA. Malnutrition and parasitic helminth infections.
558 Parasitology; 2000; 121, Suppl S23-S38. DOI: 10.1017/s0031182000006491. PMID: 11386688

559

560 4. Hall A, Hewitt G, Tuffrey V, Silva N. A review and meta-analysis of the impact of intestinal
561 worms on child growth and nutrition. Matern Child Nutr. 2008; 4 Suppl 1(Suppl 1):118-236.
562 DOI: 10.1111/j.1740-8709.2007.00127.x PMID: 18289159

563

564 5. Keiser J, Utzinger J. Efficacy of current drugs against soil-transmitted helminth infections:
565 systematic review and meta-analysis. JAMA. 2008; 299(16):1937-48. DOI:
566 10.1001/jama.299.16.1937. PMID: 18430913

567

568 6. Belizario VY, Amarillo ME, Leon WU, Reyes AE, Bugayong MG, Macatangay BJC. A
569 comparison of the efficacy of single doses of albendazole, ivermectin, and diethylcarbamazine

570 alone or in combinations against *Ascaris* and *Trichuris* spp. Bull World Health Organ. 2003;
571 81(1):35-42. PMID: 12640474
572
573 7. Albonico M, Bickle Q, Ramsan M, Montresor A, Savioli L, Taylor M. Efficacy of mebendazole
574 and levamisole alone or in combination against intestinal nematode infections after repeated
575 targeted mebendazole treatment in Zanzibar. Bull World Health Organ. 2003; 81(5):343-52.
576 PMID: 12856052
577
578 8. Tritten L, Silbereisen A, Keiser J. *In vitro* and *In vivo* efficacy of monepantel (AAD 1566)
579 against laboratory models of human intestinal nematode infections. PLoS Negl Trop Dis. 2011;
580 5(12):e1457. DOI: 10.1371/journal.pntd.0001457. PMID: 22216366
581
582 9. Steinmann P, Utzinger J, Du Z, Jiang J, Chen J, Hattendorf J, et al. Efficacy of single-dose and
583 triple-dose albendazole and mebendazole against soil-transmitted helminths and *Taenia* spp.: a
584 randomized controlled trial. PLoS One. 2011;6(9):e25003. DOI: 10.1371/journal.pone.0025003.
585 PMID: 21980373
586
587 10. Knopp S, Mohammed KA, Speich B, Hattendorf J, Khamis IS, Khamis AN, et al. Albendazole
588 and mebendazole administered alone or in combination with ivermectin against *Trichuris*
589 *trichiura*: a randomized controlled trial. Clin Infect Dis. 2010; 51(12):1420-8. DOI:
590 10.1086/657310. PMID: 21062129
591
592 11. Namwanje H, Kabatereine NB, Olsen A. Efficacy of single and double doses of albendazole and
593 mebendazole alone and in combination in the treatment of *Trichuris trichiura* in school-age

children in Uganda. Trans R Soc Trop Med Hyg. 2011; 105(10):586-90. DOI: 10.1016/j.trstmh.2011.07.009 . PMID: 21885077

12. Olsen A, Namwanje H, Nejsum P, Roepstorff A, Thamsborg SM. Albendazole and mebendazole have low efficacy against *Trichuris trichiura* in school-age children in Kabale District, Uganda. Trans R Soc Trop Med Hyg. 2009; 103(5):443-6. DOI: 10.1016/j.trstmh.2008.12.010. PMID: 19201005

13. Sangster NC, Cowling A, Woodgate RG. Ten Events That Defined Anthelmintic Resistance Research. Trends Parasitol. 2018; 34(7):553-563. DOI: 10.1016/j.pt.2018.05.001. PMID: 29803755

14. Diawara A, Halpenny CM, Churcher TS, Mwandawiro C, Kihara J, Kaplan RM, et al. Association between response to albendazole treatment and beta -tubulin genotype frequencies in soil-transmitted helminths. PLoS Negl Trop Dis. 2013; 30;7(5):e2247. DOI: 10.1371/journal.pntd.0002247. PMID: 23738029

15. Krücken J, Fraundorfer K, Mugisha JC, Ramüncke S, Sifft KC, Geus D, et al. Reduced efficacy of albendazole against *Ascaris lumbricoides* in Rwandan schoolchildren. Int J Parasitol Drugs Drug Resist. 2017; 7(3):262-271. DOI: 10.1016/j.ijpddr.2017.06.001. PMID: 28697451

16. Martin RJ, Clark CL, Trailovic SM, Robertson AP. Oxantel is an N-type (methyridine and nicotine) agonist not an L-type (levamisole and pyrantel) agonist: classification of cholinergic

anthelmintics in *Ascaris*. Int J Parasitol. 2004; 34(9):1083-90. DOI: 10.1016/j.ijpara.2004.04.014. PMID: 15313135

17. McFarland JW, Howes HL. Novel anthelmintic agents. 6. Pyrantel analogs with activity against whipworm. J Med Chem. 1972; 15(4):365-8. DOI: 10.1021/jm00274a008. PMID: 4623095

18. Sheehan DJ, Sheehan SM, Marchiondo AA. Discovery and Chemistry of Pyrantel, Morantel and Oxantel. Pyrantel Parasiticide Therapy in Humans and Domestic Animals. Edited by: Alan A. Marchiondo. Academic Press; 2016. pp. 1–19. https://doi.org/10.1016/B978-0-12-801449-3.00012-0

19. Lee EL, Iyngkaran N, Grieve AW, Robinson MJ, Dissanaike AS. Therapeutic evaluation of oxantel pamoate (1, 4, 5, 6-tetrahydro-1-methyl-2-[trans-3-hydroxystyryl] pyrimidine pamoate) in severe *Trichuris trichiura* infection. Am J Trop Med Hyg. 1976; 25(4):563-7. DOI: 10.4269/ajtmh.1976.25.563. PMID: 961973

20. Garcia EG. Treatment for trichuriasis with oxantel. Am J Trop Med Hyg. 1976 25(6):914-5. DOI: 10.4269/ajtmh.1976.25.914. PMID: 1008134

21. Speich B, Ame SM, Ali SM, Alles R, Huwyler J, Hattendorf J, et al. Oxantel pamoate-albendazole for *Trichuris trichiura* infection. N Engl J Med. 2014; 13;370(7):610-20. DOI: 10.1056/NEJMoa1301956. PMID: 24521107

640 22. Moser W, Ali SM, Ame SM, Speich B, Puchkov M, Huwyler J, et al. Efficacy and safety of
641 oxantel pamoate in school-aged children infected with *Trichuris trichiura* on Pemba Island,
642 Tanzania: a parallel, randomised, controlled, dose-ranging study. Lancet Infect Dis. 2016;
643 16(1):53-60. DOI: 10.1016/S1473-3099(15)00271-6. PMID: 26388169
644
645 23. World Health Organization. Assessing the efficacy of anthelminthic drugs against
646 schistosomiasis and soil-transmitted helminthiases. World Health Organization; 2013. Available
647 at: https://apps.who.int/iris/handle/10665/79019
648
649 24. Wolstenholme AJ, Neveu C. The interactions of anthelmintic drugs with nicotinic receptors in
650 parasitic nematodes. Emerg Top Life Sci. 2017; 1 (6): 667–673.
651 https://doi.org/10.1042/ETLS20170096
652
653 25. Albuquerque EX, Pereira EFR, Alkondon M, Rogers SW. Mammalian Nicotinic Acetylcholine
654 Receptors: From Structure to Function. Physiol Rev. Ame2009; 89(1):73-120. DOI:
655 10.1152/physrev.00015.2008. PMID: 19126755
656
657 26. HoldenDye L, Joyner M, O'Connor V, Walker RJ. Nicotinic acetylcholine receptors: a
658 comparison of the nAChRs of *Caenorhabditis elegans* and parasitic nematodes. Parasitol
659 Int.2013; 62(6):606-15. DOI: 10.1016/j.parint.2013.03.004. PMID: 2350039
660
661 27. Qian H, Martin RJ, Robertson AP. Pharmacology of N-, L-, and B-subtypes of nematode
662 nAChR resolved at the single-channel level in *Ascaris suum*. FASEB J. 2006; 20(14):2606-8.
663 DOI: 10.1096/fj.06-6264fje. PMID: 17056760

28. Ballivet M, Alliod C, Bertrand S, Bertrand D. Nicotinic Acetylcholine Receptors in the Nematode *Caenorhabditis elegans*. J Mol Biol. 1996; 258(2):261-9. DOI: 10.1006/jmbi.1996.0248. PMID: 8627624

29. Abongwa M, Buxton SK, Courtot E, Charvet CL, Neveu C, McCoy CJ, et al. Pharmacological profile of *Ascaris suum* ACR-16, a new homomeric nicotinic acetylcholine receptor widely distributed in *Ascaris* tissues. Br J Pharmacol. 2016; 173(16):2463-77. DOI: 10.1111/bph.13524. PMID: 27238203

30. Raymond V, Mongan N., Sattelle D. Anthelmintic actions on homomer-forming nicotinic acetylcholine receptor subunits: chicken α7 and ACR-16 from the nematode *Caenorhabditis elegans*. Neuroscience. 2000; 101(3):785-91. DOI: 10.1016/s0306-4522(00)00279-7. PMID: 11113327

31. Mongan NP, Jones AK, Smith GR, Sansom MSP, Sattelle DB. Novel α7-like nicotinic acetylcholine receptor subunits in the nematode *Caenorhabditis elegans.* Protein Sci. 2002; 11(5):1162-71. DOI: 10.1110/ps.3040102. PMID**:** 11967372

32. Bennett HM, Lees K, Harper KM, Jones AK, Sattelle DB, Wonnacott S, et al. *Xenopus laevis* RIC-3 enhances the functional expression of the *C. elegans* homomeric nicotinic receptor, ACR-16, in *Xenopus* oocytes. J Neurochem. 2012; 123(6):911-8. DOI: 10.1111/jnc.12013. PMID: 2297069

688 33. Charvet CL, Guégnard F, Courtot E, Cortet J, Neveu C. Nicotine-sensitive acetylcholine
689 receptors are relevant pharmacological targets for the control of multidrug resistant parasitic
690 nematodes. Int J Parasitol Drugs Drug Resist. 2018; 8(3):540-549. DOI:
691 10.1016/j.ijpddr.2018.11.003. PMID: 30502120
692
693 34. Sleigh JN. Functional analysis of nematode nicotinic receptors. Biosci Horizons, Int J Stud
694 Research. 2010;3(1):29–39. doi:10.1093/biohorizons/hzq005
695
696 35. Williamson SM, Walsh TK, Wolstenholme AJ. The cys-loop ligand-gated ion channel gene
697 family of *Brugia malayi* and *Trichinella spiralis*: A comparison with *Caenorhabditis elegans*.
698 Invertebr Neurosci. 2007; 7(4):219-26. DOI: 10.1007/s10158-007-0056-0. PMID: 17952476
699
700 36. Dale VME, Martin RJ. Oxantel-activated single channel currents in the muscle membrane of
701 *Ascaris suum*. Parasitology. 1995; 110 (Pt 4):437-48. DOI: 10.1017/s0031182000064775.
702 PMID: 7538657
703
704 37. Robertson SJ, Pennington AJ, Mark Evans A, Martin RJ. The action of pyrantel as an agonist
705 and an open channel blocker at acetylcholine receptors in isolated *Ascaris suum* muscle vesicles.
706 Eur J Pharmacol. 1994; 271(2-3):273-82. DOI: 10.1016/0014-2999(94)90784-6. PMID:
707 7535704
708
709 38. Touroutine D, Fox RM, Stetina SE von, Burdina A, Miller DM, III, et al. acr-16 Encodes an
710 essential subunit of the levamisole-resistant nicotinic receptor at the *Caenorhabditis elegans*

711 neuromuscular junction. J Biol Chem. 2005; 280(29):27013-21. DOI:
712 10.1074/jbc.M502818200. PMID: 15917232
713
714 39. Hansen CP, Jensen AA, Christensen JK, Balle T, Liljefors T, Frølund B. Novel acetylcholine
715 and carbamoylcholine analogues: Development of a functionally selective α4β2 nicotinic
716 acetylcholine receptor agonist. J Med Chem. 2008; 51(23):7380-95. DOI: 10.1021/jm701625v.
717 PMID: 18989912
718
719 40. Hansen TVA, Williams AR, Denwood M, Nejsum P, Thamsborg SM, Friis C. Pathway of
720 oxfendazole from the host into the worm: *Trichuris suis* in pigs. Int J Parasitol Drugs Drug
721 Resist. 2017; 7(3):416-424. DOI: 10.1016/j.ijpddr.2017.11.002. PMID: 29156431
722
723 41. Altschul SF, Madden TL, Sch+ñffer AA, Zhang J, Zhang Z, Miller W, et al. Gapped BLAST
724 and PSI-BLAST: a new generation of protein database search programs. Nucleic Acids Res.
725 1997; 25(17):3389-402. DOI: 10.1093/nar/25.17.3389. PMID: 9254694
726
727 42. Petersen TN, Brunak S, Von Heijne G, Nielsen H. SignalP 4.0: Discriminating signal peptides
728 from transmembrane regions. Nat Methods. 2011; 8(10):785-6. DOI: 10.1038/nmeth.1701.
729 PMID: 21959131
730
731 43. Krogh A, Larsson B, Von Heijne G, Sonnhammer ELL. Predicting transmembrane protein
732 topology with a hidden Markov model: Application to complete genomes. J Mol Biol. 2001;
733 305(3):567-80. DOI: 10.1006/jmbi.2000.4315. PMID: 11152613
734

735 44. Jespersen T, Grunnet M, Angelo K, Klærke DA, Olesen S-P. Dual-function vector for protein
736 expression in both mammalian cells and *Xenopus laevis* oocytes. Biotechniques. 2002;
737 32(3):536-8. DOI: 10.2144/02323st05. PMID: 11911656

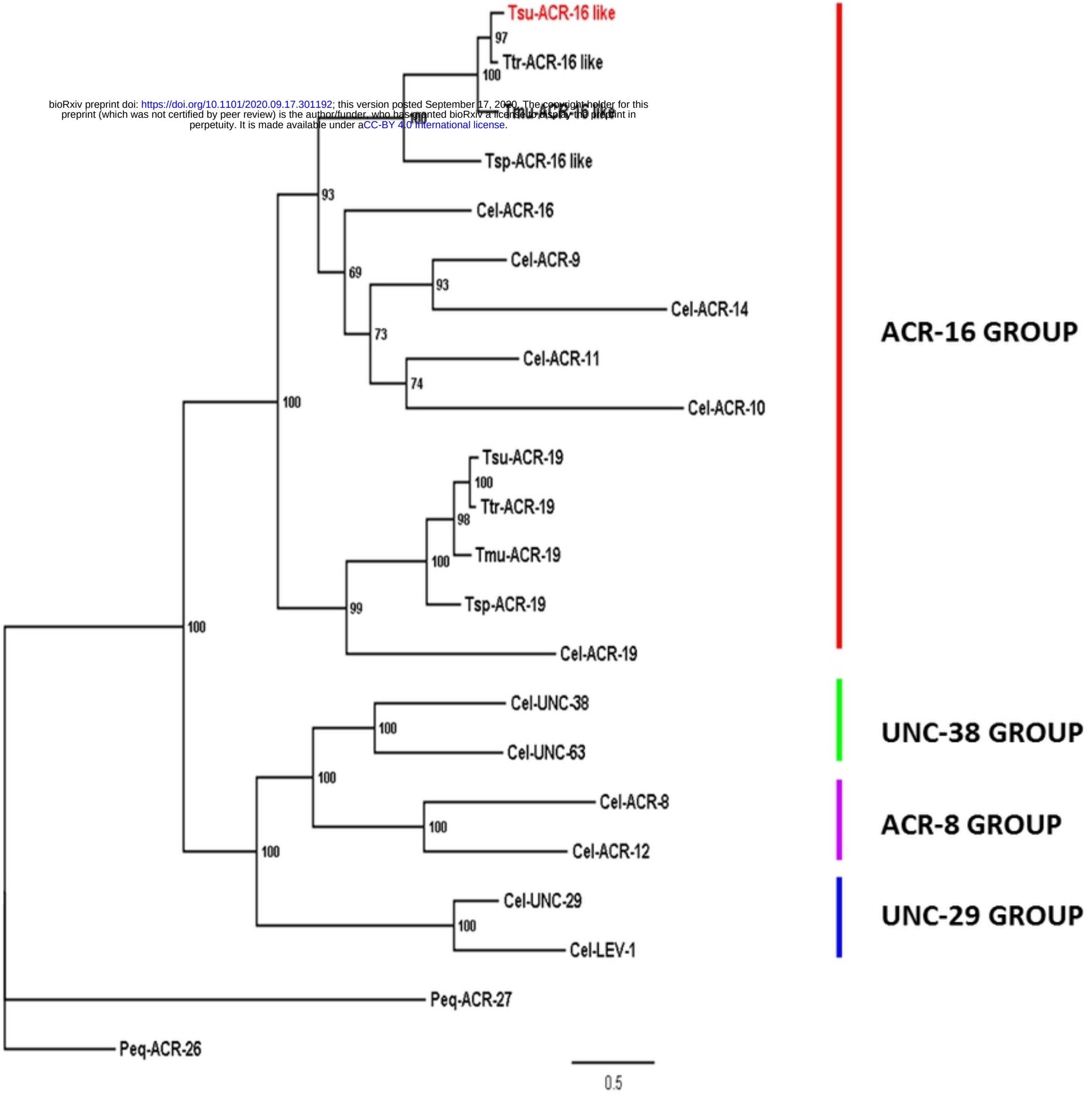

Figure

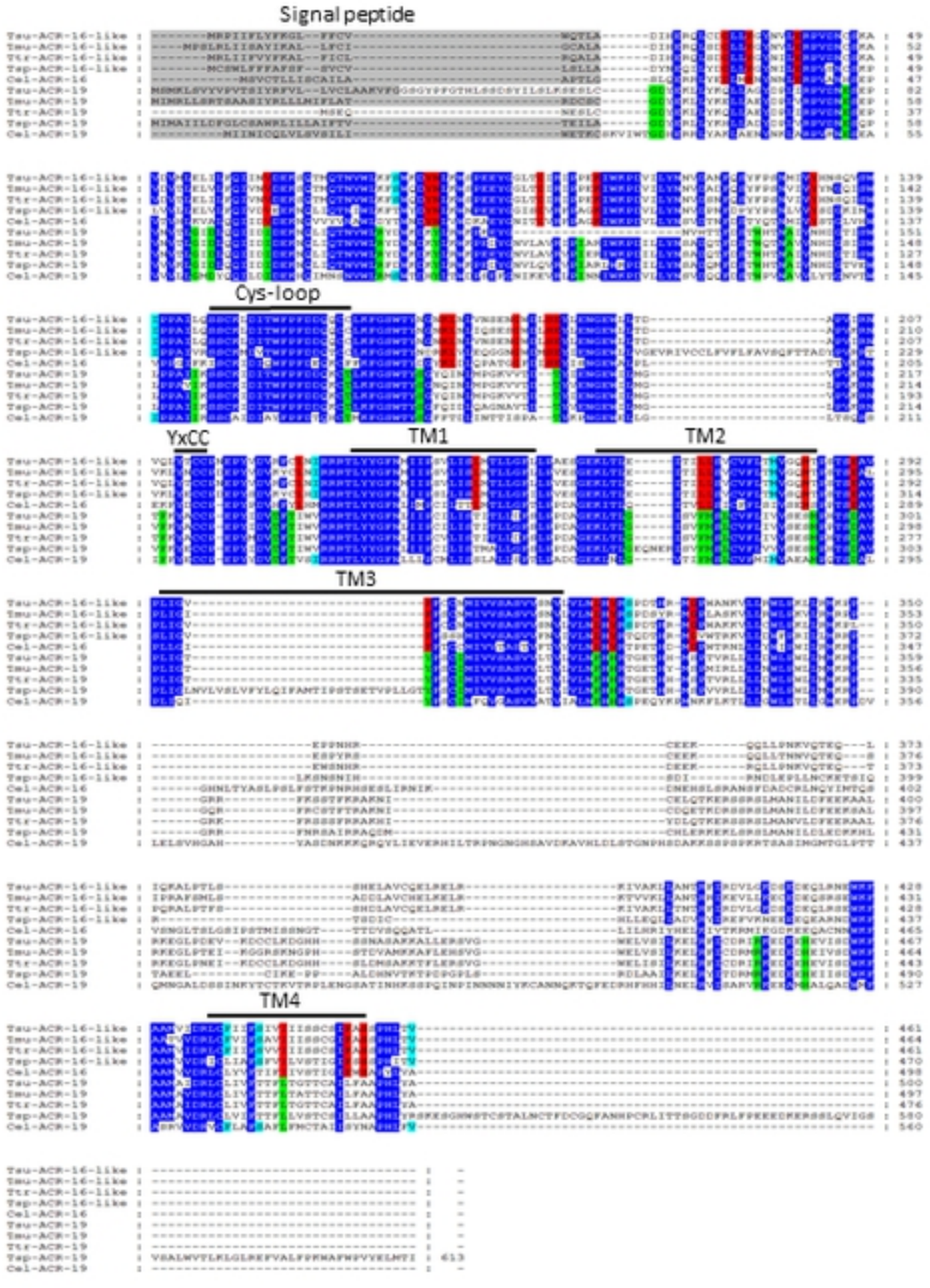

Figure

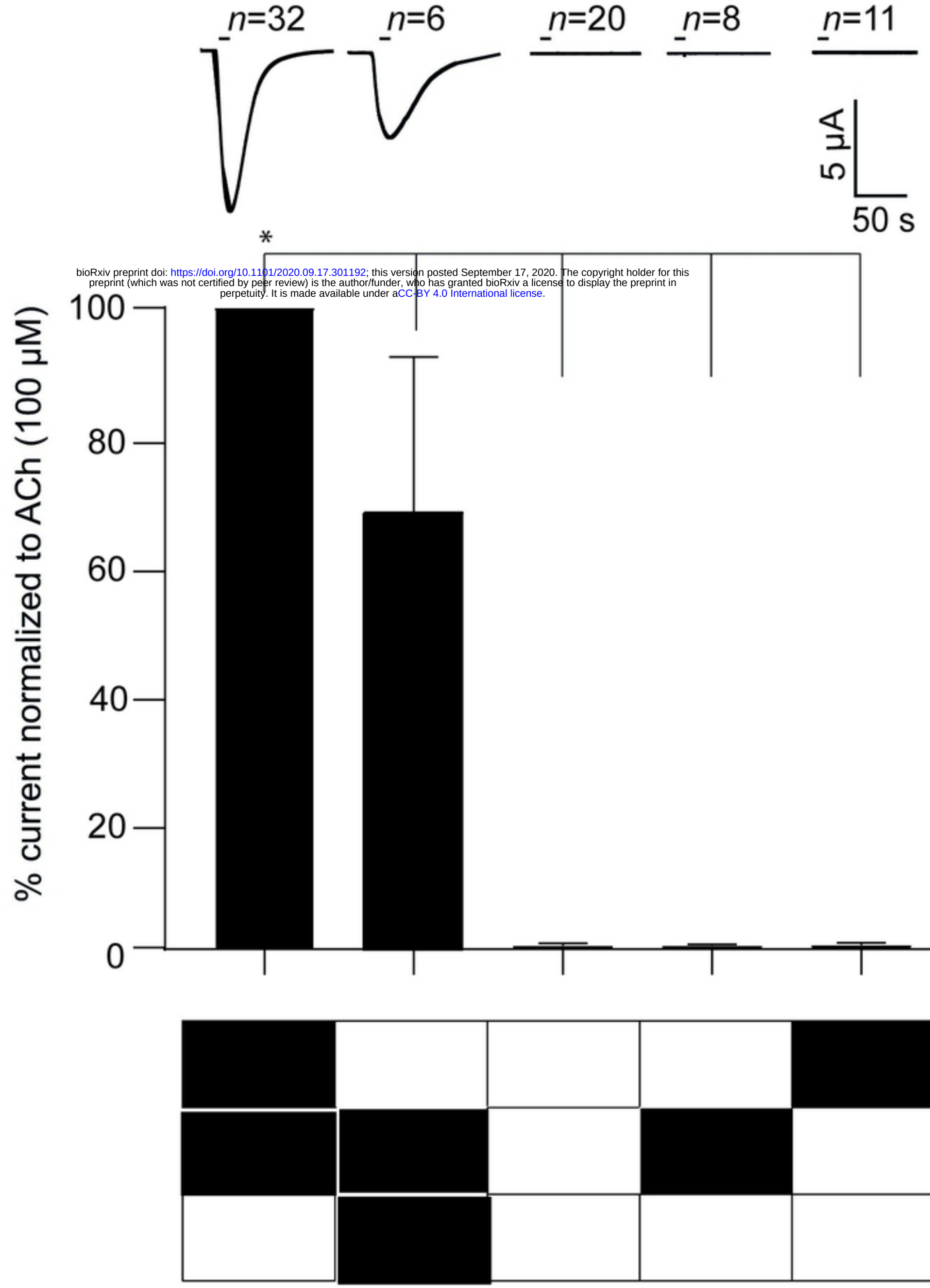

Figure

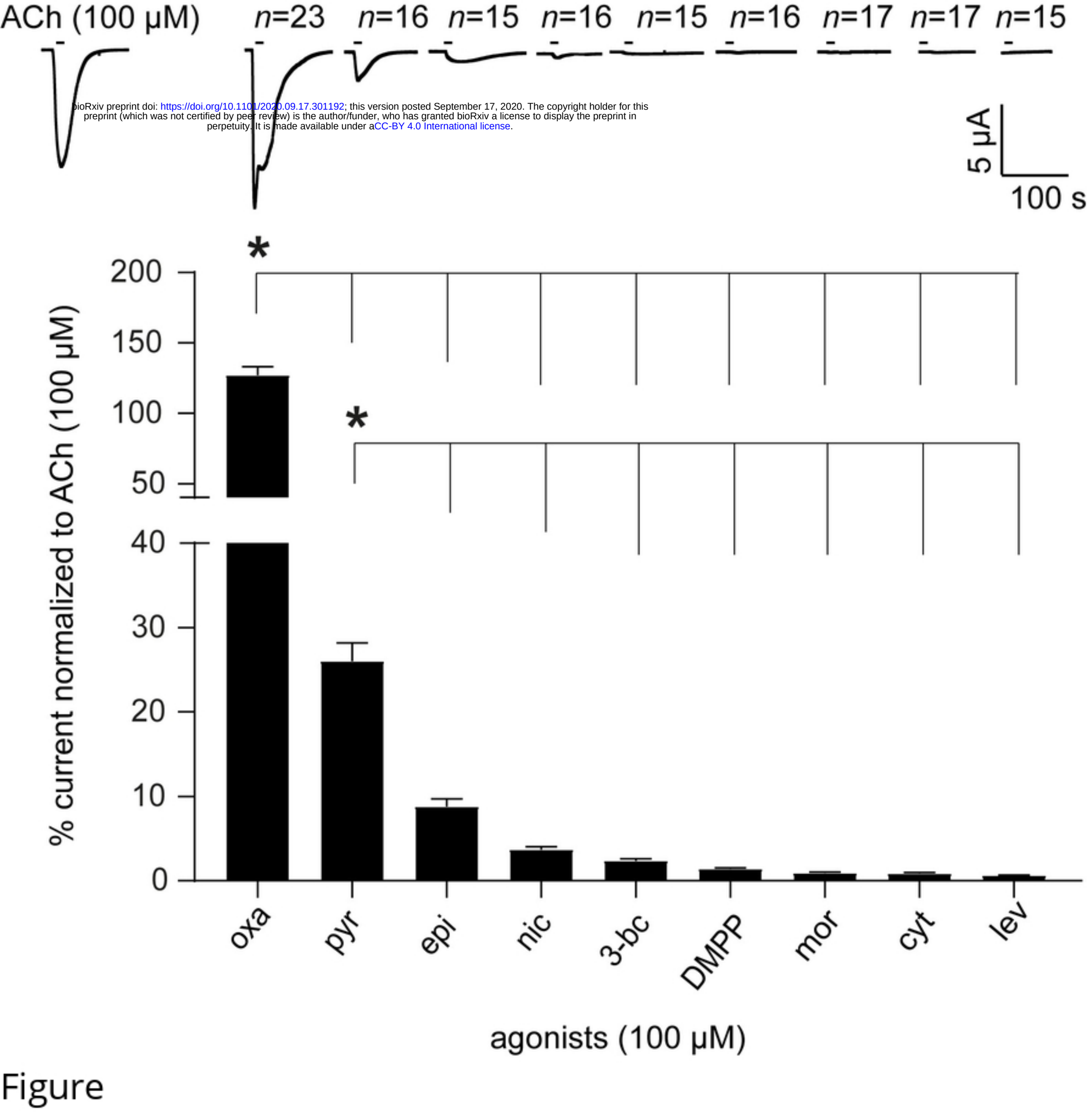

Figure

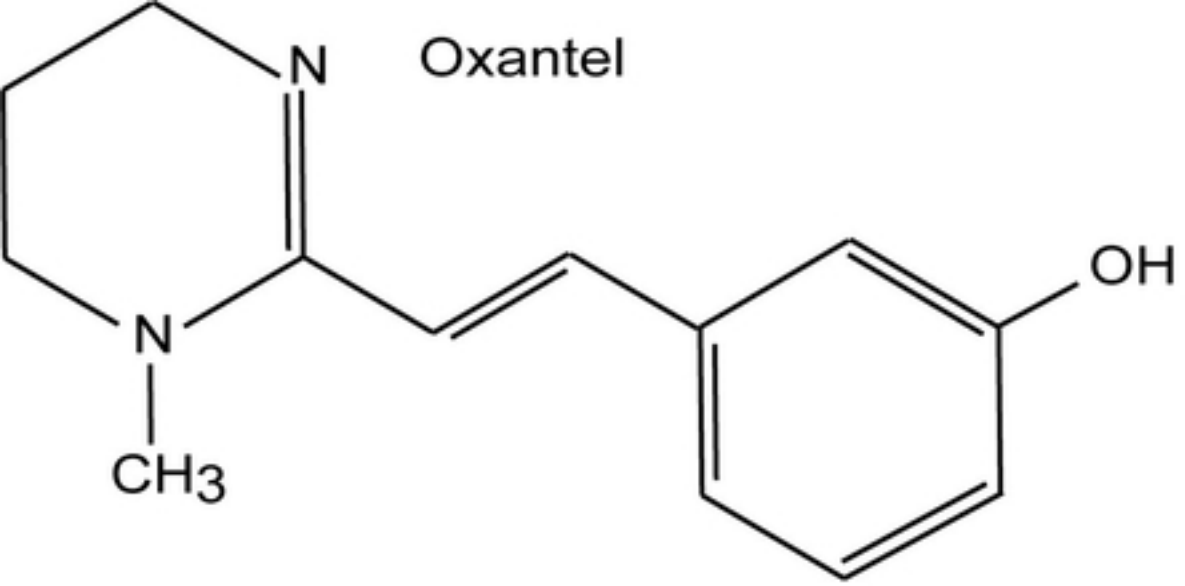

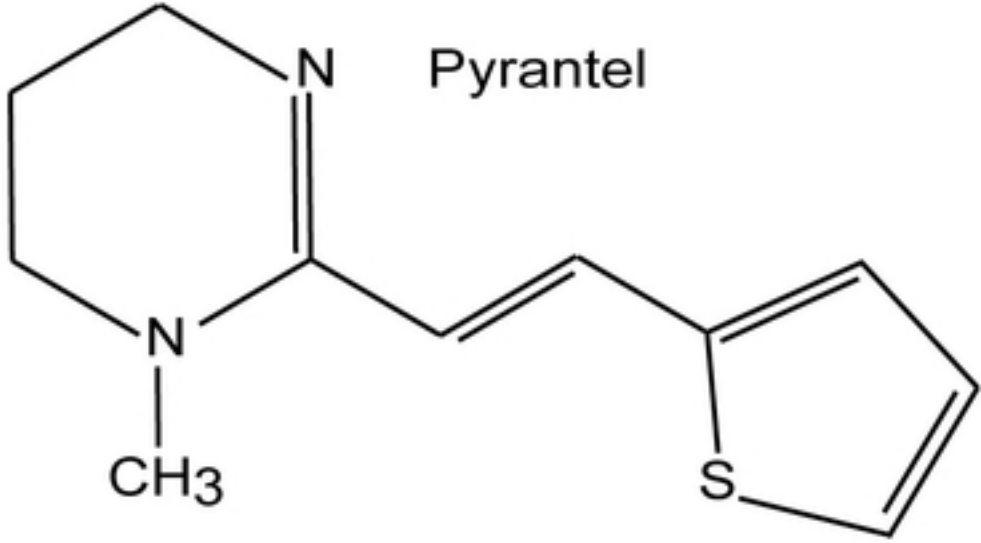

Figure

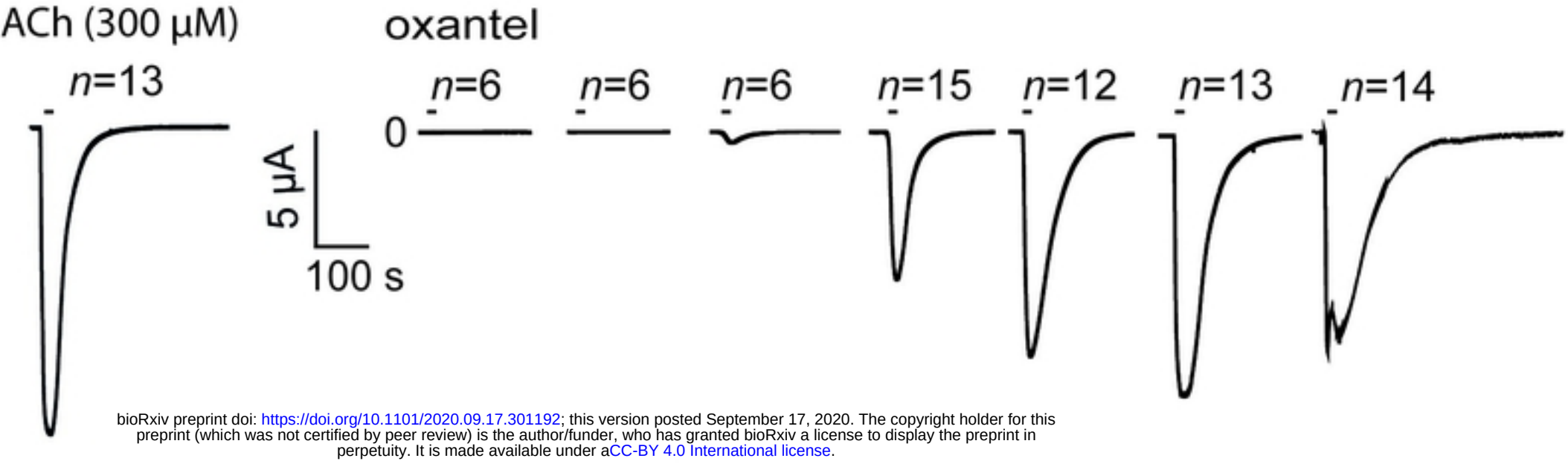

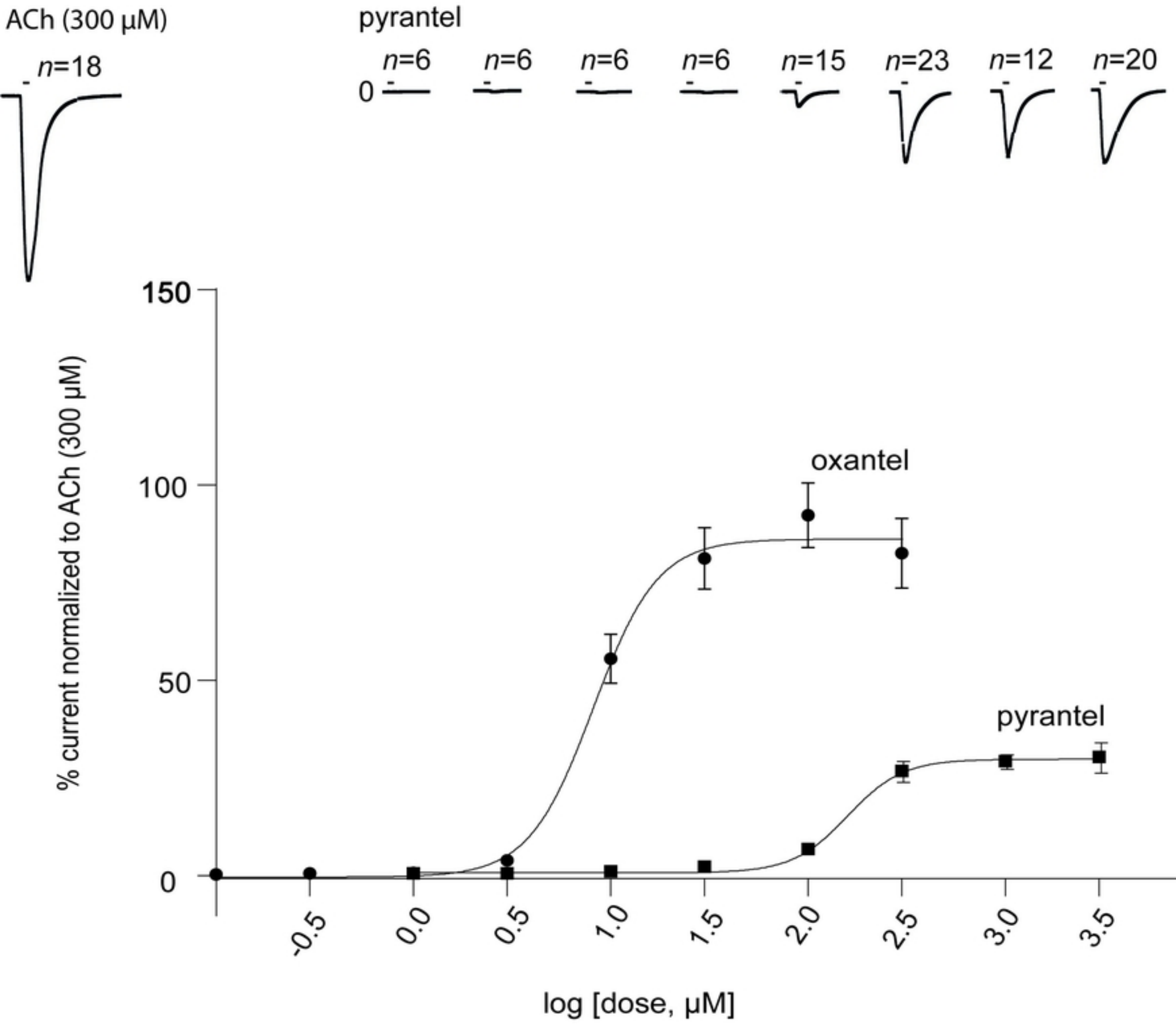

Figure

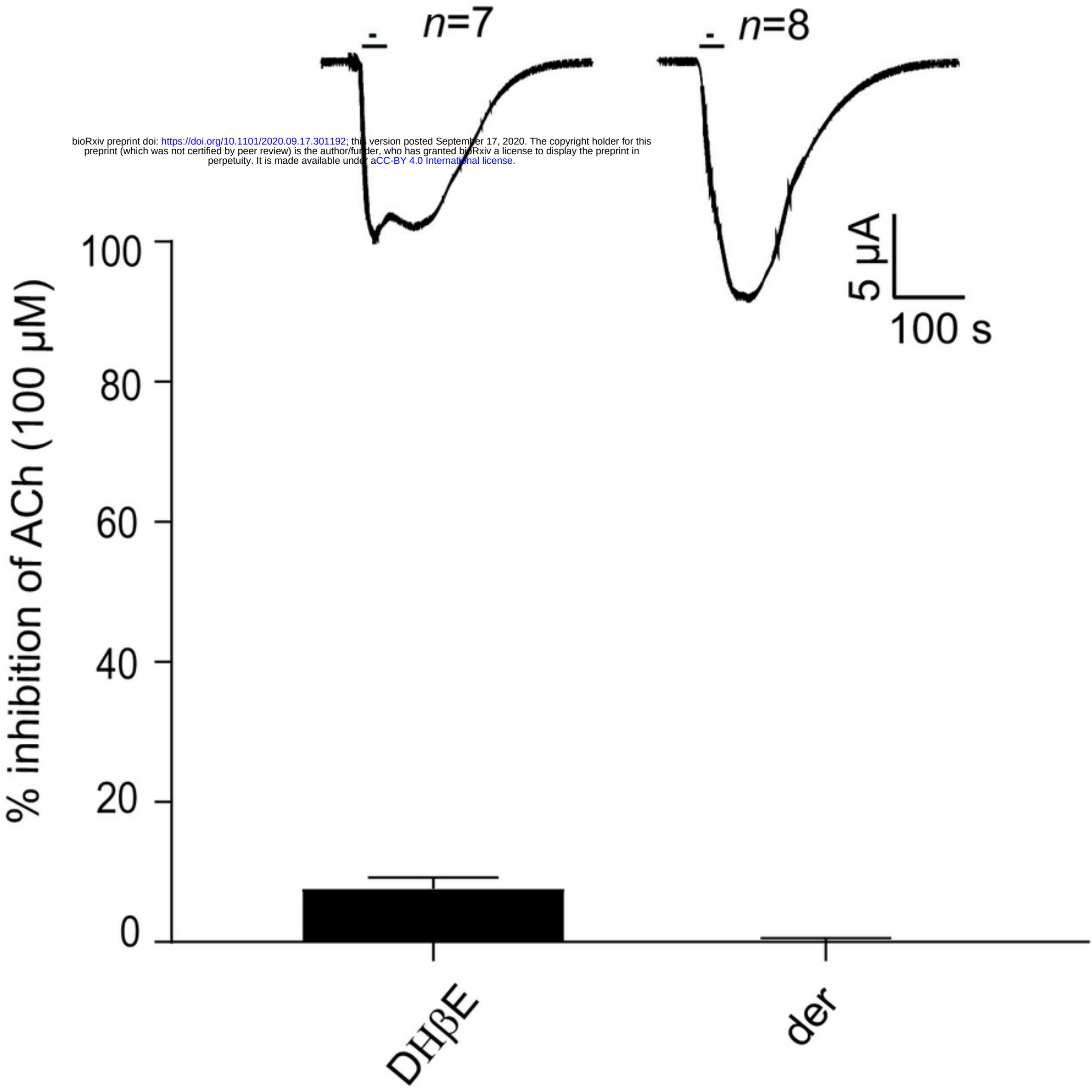

Figure

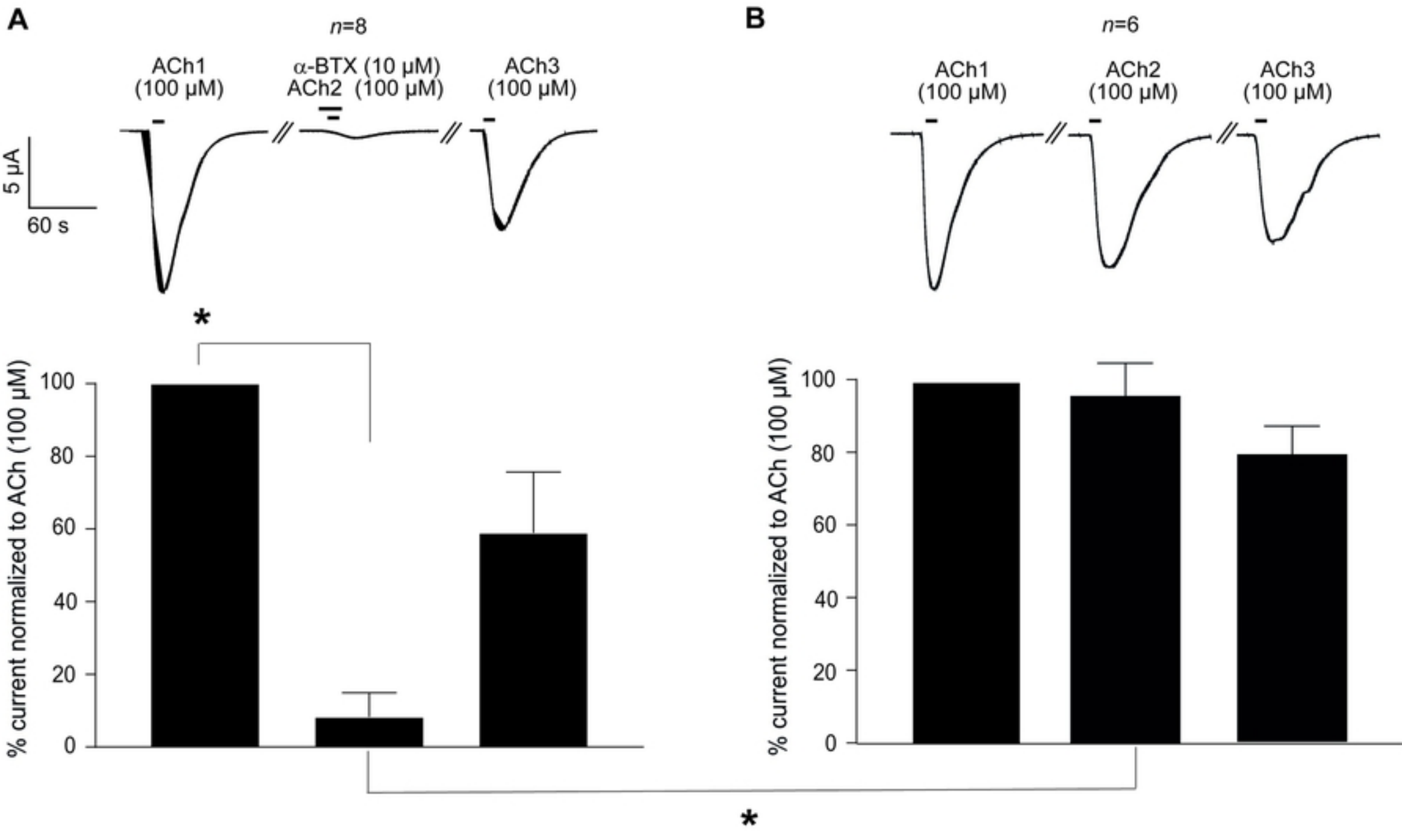
A
n=8
ACh1
(100 µM)
α-BTX (10 µM)
ACh2 (100 µM)
ACh3
(100 µM)
5 µA
60 s
*
% current normalized to ACh (100 µM)
100
80
60
40
20
0
B
n=6
ACh1
(100 µM)
ACh2
(100 µM)
ACh3
(100 µM)
% current normalized to ACh (100 µM)
100
80
60
40
20
0
*

Figure